Slow- and Fast-Binding Inhibitors of Thermolysin Display Different Modes of Binding: Crystallographic Analysis of Extended Phosphonamidate Transition-State Analogues[†]

Hazel M. Holden,[‡] Dale E. Tronrud, Arthur F. Monzingo,[§] Larry H. Weaver, and Brian W. Matthews*

Institute of Molecular Biology and Department of Physics, University of Oregon, Eugene, Oregon 97403

Received May 18, 1987; Revised Manuscript Received August 6, 1987

ABSTRACT: The modes of binding to thermolysin of two phosphonamidate peptide inhibitors, carbobenzoxy-Gly^P-L-Leu-L-Leu (ZG^{P}LL) and carbobenzoxy-L-Phe^P-L-Leu-L-Ala (ZF^{P}LA), have been determined by X-ray crystallography and refined at high resolution to crystallographic R-values of 17.7% and 17.0%, respectively. (Gly^P is used to indicate that the trigonal carbon of the peptide linkage is replaced by the tetrahedral phosphorus of a phosphonamidate group.) These inhibitors were designed to be structural analogues of the presumed catalytic transition state and are potent inhibitors of thermolysin (ZG^{P}LL, K_i = 9.1 nM; ZF^{P}LA, K_i = 0.068 nM) [Bartlett, P. A., & Marlowe, C. K. (1987) *Biochemistry* (following paper in this issue)]. ZF^{P}LA binds to thermolysin in the manner expected for the transition state and, for the first time, provides direct support for the presumed mode of binding of extended substrates in the S_2 subsite. The mode of binding of ZF^{P}LA displays all the interactions that are presumed to stabilize the transition state and supports the postulated mechanism of catalysis [Hangauer, D. G., Monzingo, A. F., & Matthews, B. W. (1984) *Biochemistry 23*, 5730–5741]. The two oxygens of the phosphonamidate moiety are liganded to the zinc to give overall pentacoordination of the metal. For the second inhibitor the situation is different. Although both ZF^{P}LA and ZG^{P}LL have similar modes of binding in the S_1' and S_2' subsites, the configurations of the carbobenzoxy-Phe and carbobenzoxy-Gly moieties are different. For ZF^{P}LA the carbonyl group of the carbobenzoxy group is hydrogen bonded directly to the enzyme, whereas in ZG^{P}LL the carbonyl group is rotated 117°, and there is a water molecule interposed between the inhibitor and the enzyme. For ZG^{P}LL only one of the phosphonamidate oxygens is liganded to the zinc. Correlated with the change in inhibitor–zinc ligation from monodentate in ZG^{P}LL to bidentate in ZF^{P}LA there is an increase in the phosphorus–nitrogen bond length of about 0.25 Å, strongly suggesting that the phosphonamide nitrogen in ZF^{P}LA is cationic, analogous to the doubly protonated nitrogen of the transition state. The observation that the nitrogen of ZF^{P}LA appears to donate two hydrogen bonds to the protein also indicates that it is cationic. The different configurations adopted by the respective inhibitors are correlated with large differences in their kinetics of binding [Bartlett, P. A., & Marlowe, C. K. (1987) *Biochemistry* (following paper in this issue)]. These differences in kinetics are not associated with any significant conformational change on the part of the enzyme. Rather, the slow-binding behavior of ZF^{P}LA and related α-substituted inhibitors is correlated with the displacement of a specific water molecule from the active site.

Thermolysin, isolated from *Bacillus thermoproteolyticus*, is a zinc-requiring endopeptidase of M_r 34 600. The three-dimensional structure of the protein is known and has been refined to a nominal resolution of 1.6 Å (Holmes & Matthews, 1982). Overall, the tertiary structure of thermolysin may be described as two spherical domains separated by a deep cleft that constitutes the active site.

It has become increasingly apparent that zinc-containing proteases are widely distributed in nature and play important roles in numerous physiological processes such as digestion and blood-pressure regulation. In an attempt to understand the catalytic mechanism of thermolysin and other related zinc proteases, a series of inhibitors of the enzyme has been studied crystallographically (Kester & Matthews, 1977; Weaver et al., 1977; Bolognesi & Matthews, 1979; Holmes & Matthews,

1981; Monzingo & Matthews, 1982, 1984; Holmes et al., 1983; Tronrud et al., 1986, 1987a). Taken together, these inhibitor studies have suggested the catalytic mechanism shown in simplified form in Figure 1 (Hangauer et al., 1984). At the presumptive transition state the hydrated carbonyl carbon of the peptide substrate is in a tetrahedral configuration and the zinc ion is pentacoordinated by three protein plus two substrate ligands, rather than three protein ligands plus a water molecule as in native thermolysin.

The concept of transition-state analogues has proven very effective as a basis for designing potent enzyme inhibitors. Such transition-state analogues are synthesized on the premise that binding interactions between an enzyme and its substrate are optimal at the transition state (Pauling, 1946; Wolfenden, 1976; Bartlett & Marlowe, 1983). Apart from their potential as antimetabolites, transition-state inhibitors can provide mechanistic information regarding enzyme catalysis (Wolfenden, 1976).

Phosphoramidon [N-[N-[[(6-deoxy-α-L-mannopyranosyl)-oxy]hydroxyphosphinyl]-L-leucyl]-L-tryptophan] is a potent, naturally occurring, inhibitor of thermolysin (Suda et al., 1973; Komiyama et al., 1975) and is presumed to be a transition-state analogue (Weaver et al., 1977). Other, simpler, phos-

*Author to whom correspondence should be addressed.

[‡] Present address: Department of Biochemistry, Biological Sciences West, University of Arizona, Tucson, AZ 85721.

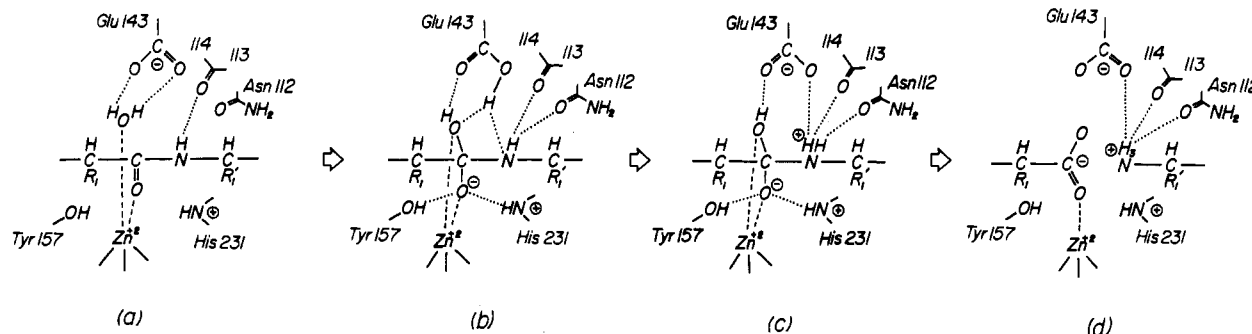[§] Present address: Department of Chemistry, University of Texas at Austin, Austin, TX 78712.

FIGURE 1: Schematic representation of the key features of the presumed mechanism of action of thermolysin. An incoming peptide is presumed to displace a zinc-bound water molecule toward Glu-143, forming a pentacoordinate complex (a). The water molecule, activated by the combined influence of the metal ion and Glu-143, attacks the carbonyl carbon to form a tetrahedral intermediate (b). The tetrahedral intermediate is presumed to form a bidentate complex with the zinc and is stabilized in part by hydrogen bonds from His-231 and Tyr-157. Glu-143 accepts the proton from the activated water molecule and is presumed to subsequently donate the proton to the scissile nitrogen (c), although proton donation by solvent water is not excluded as an alternative. Glu-143 is presumed to also shuttle the remaining proton from the hydroxyl derived from the nucleophilic water molecule to the generated primary amine to yield products (d) [after Hangauer et al. (1984)].
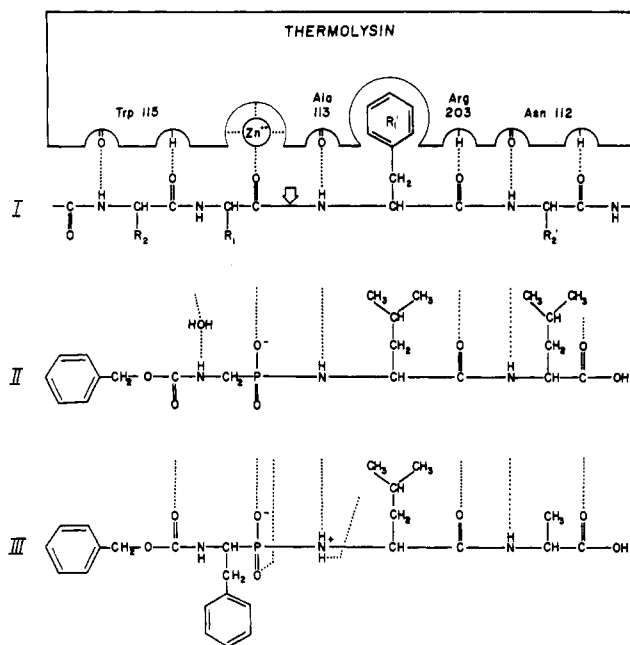

FIGURE 2: Schematic illustration showing the structures of the inhibitors ZGᴾLL (II) and ZFᴾLA (III) and some of their observed interactons with the extended thermolysin active site. (See Figure 8 for additional interactions.) The figure includes an extended substrate (I) with its presumed hydrogen bonds to the enzyme shown as dotted lines and the bond to be cleaved indicated by the arrowhead. Note the different modes of interaction of the carbobenzoxy-Gly and the carbobenzoxy-Phe groups in II and III.

phorus-containing peptide analogues have also been shown to be very effective inhibitors of the zinc peptidases (Holmquist, 1977; Kam et al., 1979; Nishino & Powers, 1979; Holmquist & Vallee, 1979; Jacobsen & Bartlett, 1981; Galardy, 1982; Thorsett et al., 1982; Galardy et al., 1983). Extending these design principles, Bartlett and Marlowe have synthesized a series of inhibitors designed specifically to mimic the geometry of an extended thermolysin substrate at the transition state (Bartlett & Marlowe, 1983, 1987). In this paper we describe the modes of binding to crystalline thermolysin of two of these inhibitors, namely, carbobenzoxy-Gly^P-L-Leu-L-Leu (ZGᴾLL) and carbobenzoxy-L-Phe^P-L-Leu-L-Ala ZFᴾLA (Figure 2). The superscript P indicates the position where the tetrahedral phosphonamide moiety replaces the planar peptide linkage. ZGᴾLL binds to thermolysin rapidly, whereas ZFᴾLA is a very slow binder (Bartlett & Marlowe, 1987). The crystallographic analysis shows that ZFᴾLA binds in the active site in the mode predicted for extended thermolysin substrates (Kester &

Table I: Intensity Statistics for ZGᴾLL and ZFᴾLA

	ZGᴾLL	ZFᴾLA
no. of films	28	27
av $R_{sym}{}^a$ (%)	3.3	2.7
av $R_{sca}{}^a$ (%)	6.4	4.8
$R_{merge}{}^a$ (%)	5.6	4.2
total reflections measured	72 525	58 214
independent reflections	31 799	28 875
resolution (Å)	1.6	1.7
av isomorphous difference (%)	16.5	11.5
cell dimensions		
a, b (Å)	94.1	93.8
c (Å)	132.0	131.9

$^a R = \sum |I - \bar{I}| \sum I$. R_{sym} measures the agreement between symmetry-related reflections on the same film, R_{sca} measures the agreement between reflections recorded on successive films in a given film pack, and R_{merge} gives the overall agreement between intensities measured on different films.

Matthews, 1977; Hangauer et al., 1984). In contrast, ZGᴾLL adopts a different configuration with a water molecule interposed between the enzyme and the bound inhibitor. It is proposed that the displacement of this solvent molecule is the rate-limiting step in the binding of ZFᴾLA.

EXPERIMENTAL PROCEDURES

Thermolysin from Calbiochem was crystallized by the method of Holmes and Matthews (1982). The crystals grow as hexagonal rods and belong to the space group P6₁22 with one monomer per asymmetric unit. They are stored in a mother liquor of 10 mM calcium acetate, 10 mM tris(hydroxymethyl)aminomethane (Tris), 7% (v/v) DMSO, pH 7.2. The unit-cell dimensions of native thermolysin crystals are $a = b = 94.2$ Å, $c = 131.4$ Å. The two inhibitors used in this study were gifts from Drs. C. K. Marlowe and P. A. Bartlett.

To prepare enzyme–inhibitor complexes, native thermolysin crystals were soaked at 4 °C for a period of several days in either 10 mM ZGᴾLL or 0.1 mM ZFᴾLA dissolved in mother liquor. The lower concentration of ZFᴾLA was used because of the tendency of the crystals to crack when exposed to this inhibitor. Cracking of this sort has been observed in previous studies and is most obvious when the crystals are first exposed to the inhibitor. After being left overnight, the crystals appear to "anneal", and many of the cracks disappear. Transient cracking could be due to changes in the unit-cell dimensions (Table I) as the inhibitor binds initially at the crystal surface. Annealing could occur as the inhibitor diffuses uniformly through the crystal. Inhibitor binding was monitored by calculating (h0l) difference Fourier projection maps from
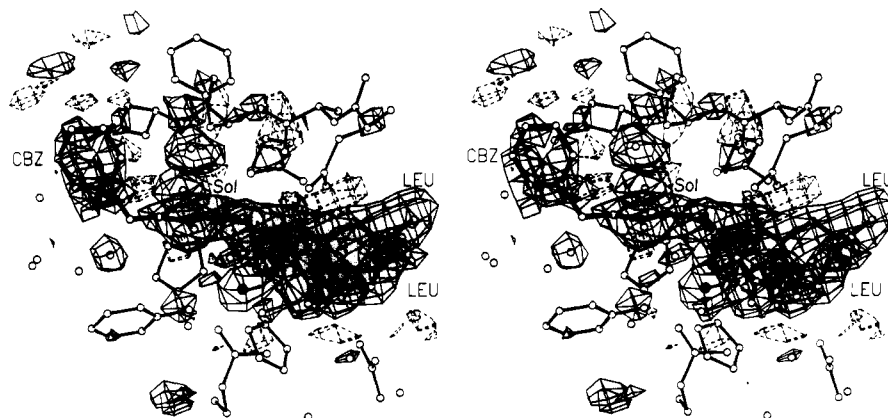
FIGURE 3: Difference electron density map, resolution 1.9 Å, with coefficients $F_{complex} - F_{nat.,calcd}$ superimposed on the model for ZG^{P}LL (shown with thick bonds). The native amplitudes and phases were calculated from the refined native structure with active-site solvent molecules removed. Positive contours (solid) and negative contours (broken) are drawn at levels of approximately 3σ and -3σ, where σ is the root mean square density throughout the unit cell. The solvent molecule that remains in place when ZG^{P}LL binds, but is displaced by ZF^{P}LA (see text), is indicated. The inhibitor is drawn with thick bonds, and adjacent protein atoms are drawn with thin bonds. The zinc ion is drawn solid. The direction of view is the same as in Figure 5.
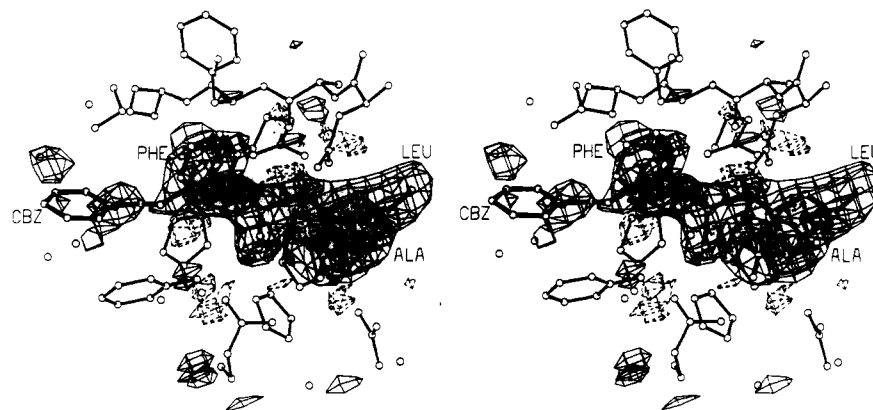

FIGURE 4: Difference electron density map for ZF^{P}LA bound to thermolysin. Details as in Figure 3.

precession photographs (Weaver et al., 1977).

A three-dimensional data set was collected for each enzyme–inhibitor complex by the method of oscillation photography (Rossmann, 1979; Schmid et al., 1981). The X-ray source was a graphite-monochromatized Elliot GX-21 rotating anode generator operated at 39 kV and 120 mA. An oscillation angle of 1.2° per film pack was used, and the crystal was rotated about the c axis through a net rotation of 30°. The typical exposure time was 4 or 6 h per film pack. Making an appropriate translation allowed a single crystal to be used for each data set. Data to 1.6-Å resolution were measured for the thermolysin–ZG^{P}LL complex and to 1.7-Å resolution for the thermolysin–ZF^{P}LA complex. Data collection statistics are summarized in Table I.

Difference electron density maps with amplitudes of the form $F_{complex} - F_{nat.,calcd}$ and phases calculated from the refined native structure clearly showed the respective inhibitors binding in the thermolysin active site cleft with the electron-dense phosphorus atom adjacent to the zinc (Figures 3 and 4). The height of the peak corresponding to the phosphorus was 17σ for ZG^{P}LL and 10σ for ZF^{P}LA, where σ is the root mean square value of the difference density throughout the unit cell. [Difference density maps with coefficients of the form $F_{complex} - F_{nat.,obsd}$ also show inhibitor binding, but their interpretation is confused by the displacement of solvent molecules [cf. Kester and Matthews (1977)].]

Initial coordinates for each inhibitor were obtained by modeling the inhibitor into the electron density on an Evans and Sutherland PS330 graphics system. Electron density maps used for the initial model-building studies were based on

Table II: Refinement Statistics for Thermolysin–Inhibitor Complexes

	ZG^{P}LL	ZF^{P}LA
resolution limits (Å)	10.0–1.6	10.0–1.7
initial R factor[a] (%)	24.9	21.6
final R factor (%)	17.7	17.0
no. of cycles	28	24
no. of reflections used	31 627	28 691
no. of atoms	2 643	2 635
weighted root mean square deviations from ideality		
bond length (Å)	0.022	0.023
bond angle (deg)	2.8	3.2
planarity (trigonal) (Å)	0.010	0.012
planarity (other planes) (Å)	0.014	0.015
torsion angle (deg)	16.4[b]	16.5[b]

[a] R factor $= \sum |F_{obsd} - F_{calcd}| / \sum |F_{obsd}|$. [b] The torsion angles were not restrained during refinement.

$2F_{complex} - F_{nat.,calcd}$ coefficients. Starting coordinates for refinement were these crude coordinates plus the coordinates of native thermolysin refined to 1.6-Å resolution (Holmes & Matthews, 1982). Refinement of the thermolysin–inhibitor complexes was carried out by using the "TNT" system of programs written and developed in this laboratory (Tronrud et al., 1987b). These programs are based on the method of restrained least squares. Occasionally during the course of the refinement, electron density maps based on $F_{complex} - F_{calcd}$ coefficients were checked for possible water molecules missing from the initial protein:inhibitor coordinates. "Ideal" stereochemistry for the protein and the inhibitor was based on the values in the TNT refinement package (Tronrud et al., 1987b)

Table III: Coordinates for ZG^PLL

atom	X (Å)	Y (Å)	Z (Å)	B (Å²)
carbobenzoxy				
OA	49.4	18.8	−9.9	28.1
CB	48.9	18.3	−11.2	29.9
CG	47.5	19.0	−11.6	25.9
CD1	46.5	19.0	−10.7	26.5
CE1	45.3	19.6	−11.0	25.0
CZ	45.1	20.3	−12.1	23.4
CE2	46.2	20.4	−13.0	26.7
CD2	47.4	19.8	−12.7	29.5
C	49.7	17.9	−8.9	20.9
O	49.6	16.7	−9.0	20.4
glycine				
N	50.1	18.6	−7.9	10.7
CA	50.4	18.0	−6.7	3.8
phosphonamide				
P	51.7	19.0	−6.1	9.7
OP1	53.1	18.6	−6.6	9.8
OP2	51.5	20.5	−6.1	10.6
N	51.7	18.5	−4.5	2.6
leucine				
CA	52.8	18.2	−3.6	13.4
CB	52.5	18.3	−2.1	5.6
CG	53.7	18.2	−1.2	11.5
CD1	54.6	19.4	−1.4	10.5
CD2	53.2	18.1	0.2	7.7
C	53.5	16.9	−3.9	19.9
O	54.8	16.8	−3.8	9.2
N	52.7	15.9	−4.2	11.7
leucine				
CA	53.2	14.5	−4.5	20.3
CB	53.5	13.7	−3.1	11.7
CG	52.3	13.5	−2.3	17.8
CD1	52.3	14.5	−1.2	23.6
CD2	52.3	12.2	−1.5	24.7
C	52.4	13.8	−5.5	22.0
O	51.3	14.5	−5.9	11.4
OH	52.8	12.8	−6.1	18.8

Table IV: Coordinates for ZF^PLA and Discrepancy with ZG^PLL[a]

atom	X (Å)	Y (Å)	Z (Å)	Δr (Å)	B (Å²)	ΔB (Å²)
carbobenzoxy						
OA	50.8	20.6	−9.9	2.3	36.8	9
CB	51.0	21.9	−10.4	4.2	28.9	−1
CG	50.5	21.8	−11.8	4.0	35.8	10
CD1	50.4	20.6	−12.6	4.6	40.1	14
CE1	49.9	20.6	−13.9	5.5	35.9	11
CZ	49.5	21.7	−14.5	5.1	34.7	11
CE2	49.5	22.8	−13.7	4.1	36.7	10
CD2	50.0	22.9	−12.4	4.1	45.5	16
C	50.4	20.4	−8.6	2.6	34.3	13
O	49.9	21.3	−7.8	4.7	14.8	−6
phenylalanine						
CB	50.7	17.2	−7.0		13.7	
CG	49.4	16.8	−7.7		21.8	
CD1	48.2	16.8	−6.9		18.6	
CE1	47.0	16.5	−7.5		29.1	
CD2	49.3	16.6	−9.0		24.6	
CE2	48.1	16.3	−9.6		28.5	
CZ	46.9	16.2	−8.8		30.9	
N	50.8	19.1	−8.2	0.9	22.5	12
CA	50.7	18.6	−6.8	0.7	15.6	12
phosphoramide						
P	52.0	19.2	−6.1	0.4	21.7	12
OP1	53.3	18.5	−6.7	0.3	16.8	7
OP2	52.1	20.7	−5.9	0.7	20.5	10
N	51.7	18.5	−4.3	0.2	10.7	8
leucine						
CA	52.9	18.3	−3.5	0.2	19.6	6
CB	52.6	18.5	−2.0	0.2	11.4	6
CG	53.8	18.4	−1.1	0.2	18.7	7
CD1	54.7	19.7	−1.3	0.4	11.0	0
CD2	53.2	18.2	0.3	0.1	14.5	7
C	53.6	17.0	−3.6	0.3	21.3	1
O	54.9	16.9	−3.6	0.2	13.7	4
N	52.9	15.9	−3.8	0.4	15.4	4
alanine						
CA	53.3	14.5	−3.9	0.6	19.5	−1
CB	53.0	13.8	−2.6	0.7	14.2	3
C	52.7	13.8	−5.1	0.6	27.6	6
O	51.7	14.3	−5.6	0.4	23.9	13
OH	53.1	12.8	−5.7	0.5	37.9	19

[a] Coordinates are in angstroms in the standard orthogonal thermolysin coordinate system (Matthews et al., 1974). B is the crystallographic thermal parameter. Δr and ΔB are the differences between the atomic positions and the thermal factors for ZF^PLA and ZG^PLL.

as well as bond lengths and angles from Bowen et al. (1958) and Kojima et al. (1978). Results from the refinement are presented in Tables II–IV, and the refined coordinates for the thermolysin–inhibitor complexes have been deposited in the Brookhaven Data Bank.

RESULTS

Binding of Inhibitors to Crystalline Thermolysin. The observed binding of ZG^PLL in the thermolysin active site is shown in Figure 5. As expected, the inhibitor binds in an extended conformation with the two leucine residues occupying the S_1' and S_2' specificity pockets. The zinc:phosphonamide–oxygen distances are 3.0 and 2.1 Å. Additional details of the geometry of the zinc ligands are given in Table V. Relevant protein:inhibitor contacts are given in Table VI.

Figure 6 shows stereographically the binding of ZF^PLA to thermolysin. Again, relevant protein:inhibitor contacts are give in Tables VI and VII. Like ZG^PLL, ZF^PLA binds to the enzyme with its phosphonamide oxygens close to the zinc and the leucine and alanine residues occupying the S_1' and S_2' subsites, respectively. However, in the case of ZF^PLA, the coordination of the zinc by the phosphonamide oxygens is decidedly bidentate with zinc:oxygen distances of 2.2 and 2.6 Å.

As can be seen in Figure 7, the R_1' and R_2' residues of both inhibitors bind to thermolysin in nearly the same orientation, and replacement of leucine by alanine in ZF^PLA makes little difference to the mode of binding in the S_1' and S_2' subsites. However, as can also be seen from Figure 7 and is shown schematically in Figure 2, ZG^PLL and ZF^PLA bind to thermolysin in a completely different orientation with respect to their carbobenzoxy moieties. In fact, the dihedral angle de-

Table V: Zinc–Ligand Geometry

ligand	distance in ZG^PLL complex (Å)	distance in ZF^PLA complex (Å)
His-142 NE2	2.04	2.09
His-146 NE2	2.09	2.11
Glu-166 OE1	2.07	2.04
inhibitor OP1	2.08	2.17
inhibitor OP2	3.01	2.59

Table VI: Selected Thermolysin–Inhibitor Distances[a]

protein	inhibitor ZG^PLL	inhibitor ZF^PLA	distance (Å) ZG^PLL	distance (Å) ZF^PLA
Trp-115 NH	Sol-362	Cbz O	2.8 (H)	3.0 (H)
Tyr-157 OH	Gly NH	Phe NH	3.9	3.3 (H)
Tyr-157 OH	OP1	OP1	3.4	3.1 (H)
His-231 NE2	OP1	OP1	2.9 (H)	2.7 (H)
Glu-143 OE1	OP2	OP2	2.5 (H)	2.3 (H)
Glu-143 OE2	Leu(1) N	Leu N	3.4	3.3
Ala-113 O	Leu(1) N	Leu N	3.0 (H)	2.9 (H)
Asn-112 OD1	Leu(1) N	Leu N	3.3	3.0 (H)
Arg-203 NH1	Leu(1) O	Leu O	3.0 (H)	2.8 (H)
Arg-203 NH2	Leu(1) O	Leu O	3.0 (H)	2.9 (H)
Asn-112 OD1	Leu(2) N	Ala N	3.2 (H)	3.1 (H)
Asn-112 ND2	Leu(2) O	Ala O	3.0 (H)	3.0 (H)

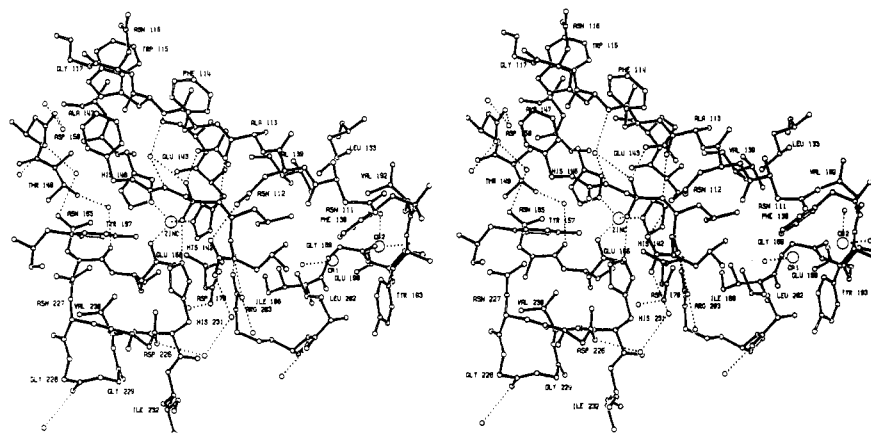[a] (H) indicates a presumed hydrogen bond.

FIGURE 5: Stereo drawing showing the mode of binding of ZG^{P}LL in the extended thermolysin active-site cleft. The inhibitor and the main-chain bonds of the protein are drawn solid; protein side chains have open bonds. Apparent hydrogen bonds between the inhibitor and the protein are shown as dotted lines. A number of bound water molecules are also included.
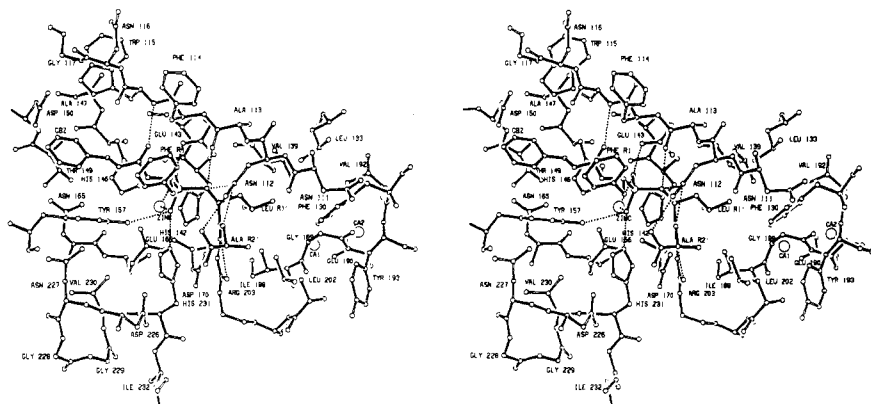

FIGURE 6: Binding of ZF^{P}LA to thermolysin (cf. Figure 5).

Table VII: Geometry of Different Phosphonamide Inhibitors of Thermolysin

inhibitor	zinc–ligand distance (Å)		liganding asymmetry [(OP2 − OP1)/(OP2 + OP1)]	P–N bond length (Å)	P–N–C angle (deg)	nitrogen protein distances (Å)			ref
	OP1	OP2				Asn-112	Ala-113	Glu-143	
phosphoramidon	1.75	3.40	0.32	1.42	128	3.4	3.4	3.9	Tronrud et al. (1986)
ZG^{P}LL (1)	2.08	3.01	0.18	1.66	129	3.3	3.0	3.4	this work
ZG^{P}LL (2)^a	1.90	3.17	0.22	1.71	121	3.2	3.0	3.5	this work
P-Leu-NH$_2$ (1)	2.06	2.79	0.15	1.85	122	3.1	3.0	3.4	Tronrud et al. (1986)
P-Leu-NH$_2$ (2)^a	1.96	2.83	0.18	1.84	126	3.7^b	3.0	3.2	Tronrud et al. (1986)
ZF^{P}LA	2.17	2.59	0.09	1.90	115	3.0	3.0	3.3	this work

^{a}The repeated entries in the table were obtained from independent refinements of these inhibitors by two different procedures. In the first case the thermolysin–inhibitor complex was refined by "TNT", a restrained least-squares procedure (Tronrud et al., 1987b). The alternative refinement was by "EREF", a combined energy minimization–crystallographic refinement procedure (Jack & Levitt, 1971). These refinement programs are different in their overall philosophy. Also, their dictionaries of "standard geometry" are different. In addition, the intensity data were remeasured between the two refinements, and the resolution was extended from 1.9 Å for EREF to 1.7 or 1.6 Å for TNT. A comparison of the repeated observations gives an impression of the uncertainty due to the limitations of the refinement. ^{b}The side chain of Asn-112 is in a slightly different conformation in the EREF model. We believe that the TNT model has the correct configuration.

fined by the N–C$_\alpha$ bond of inhibitor residue R$_1$ differs between the two analogues by 117°.

There are changes in the positions of some residues within the active site when the respective inhibitors bind, but these appear as relatively minor structural adjustments rather than distinct changes in conformation. The root mean square difference between the refined coordinates of native thermolysin and ZF^{P}LA:thermolysin is 0.18 Å, between native thermolysin and the ZG^{P}LL complex is 0.20 Å, and between one complex and the other is 0.18 Å. The largest differences between the refined coordinates of the ZF^{P}LA–thermolysin complex and native thermolysin are 0.7–0.9 Å for atoms within the side chains of residues 9, 230, and 278. These residues are some distance from the active-site region, and the dif-

ferences may simply reflect imprecision in the determination of these particular coordinates. When ZG^{P}LL binds, the largest adjustments (0.7–1.0 Å) occur for atoms within residues 115–118. In this case the shifts are confirmed by the electron density difference map (Figure 3) and correspond to a concerted "upward" movement of residues 114–118 (Figures 3 and 5).

DISCUSSION

Mode of Binding of Extended Substrates. Previous crystallographic analyses of the binding of peptide-analogue inhibitors to thermolysin have illustrated how extended substrates bind in the S$_1$, S$_1'$, and S$_2'$ subsites [e.g, see Weaver et al. (1977), Holmes and Matthews (1981), and Monzingo and
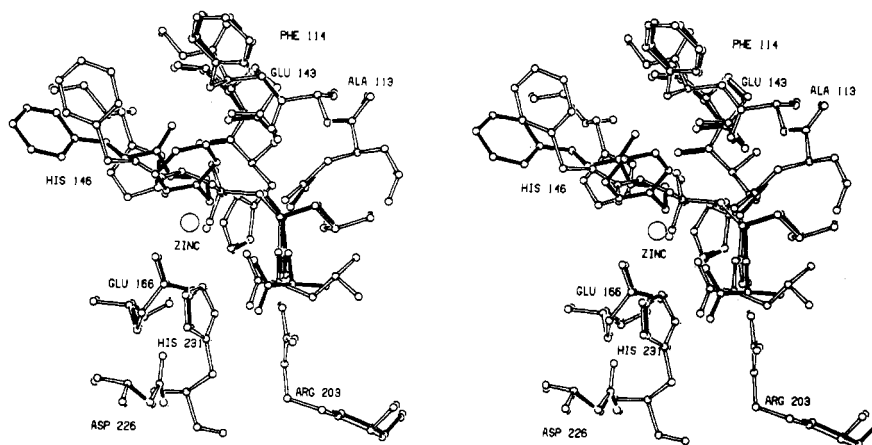
FIGURE 7: Superposition of ZG^{P}LL (open bonds) and ZF^{P}LA (solid bonds), each in its binding configuration. The corresponding refined protein structures are also superimposed.

Matthews (1982, 1984)]. In a model first proposed by Kester and Matthews (1977) and elaborated by Hangauer et al. (1984), it was suggested that in the S_1–S_2 subsites the polypeptide backbone of the substrate hydrogen bonds with the protein backbone of Trp-115 as in an antiparallel β-sheet (Figure 2). The binding of ZF^{P}LA provides the first experimental support for this proposed mode of interaction. In particular, the carbonyl oxygen of the inhibitor carbobenzoxyl moiety makes a good hydrogen bond (2.9 Å) with the peptide nitrogen of Trp-115 (Figure 6). In order to achieve this mode of binding a water molecule (Sol-362), which, in the native enzyme, hydrogen bonds to the peptide nitrogen of Trp-115 and possibly to the carboxylate of Glu-143 as well, is expelled from the active site.

In the case of ZG^{P}LL, however, the interactions with the enzyme in the S_2 subsite are very different. In this case the carbonyl oxygen of the inhibitor points away from the amide of Trp-115. The water molecule, Sol-362, is not displaced and forms a hydrogen-bonded bridge between the amide nitrogen of the inhibitor R_1 residue and the amide of Trp-115. This water molecule is discussed in more detail under Kinetics of Binding.

Mechanism of Catalysis. A mechanism for the cleavage of peptides by thermolysin was first proposed by Pangburn and Walsh (1975) and by Kester and Matthews (1977) and has been elaborated by Holmes and Matthews (1981), Monzingo and Matthews (1984), and Hangauer et al. (1984) [see also Antonov et al. (1981) and Kunugi et al. (1982)]. According to the mechanism based on these studies and outlined in Figure 1, the carbonyl oxygen of the incoming substrate coordinates to the zinc ion of the protein. The water molecule, normally the fourth ligand to the zinc in native thermolysin, is displaced toward Glu-143 but is not totally excluded from the zinc coordination sphere. There is then a nucleophilic attack by the water molecule on the carbonyl carbon of the substrate. The attacking water molecule is thought to be activated by interactions with both Glu-143 and the zinc ion. Recent studies (Monzingo & Matthews, 1984; Hangauer et al., 1984) suggest that Glu-143 accepts a proton from the attacking water molecule and shuttles this proton to the leaving nitrogen. In the presumed transition state the carbonyl carbon of the substrate is tetrahedral and the zinc ion is coordinated to five ligands rather than four as in the ground state. As discussed below, the observed mode of binding of ZF^{P}LA to thermolysin provides support for several aspects of the proposed mechanism.

ZF^{P}LA is the tightest binding inhibitor of thermolysin described to date (K_i = 0.068 nM; Bartlett & Marlowe, 1987),
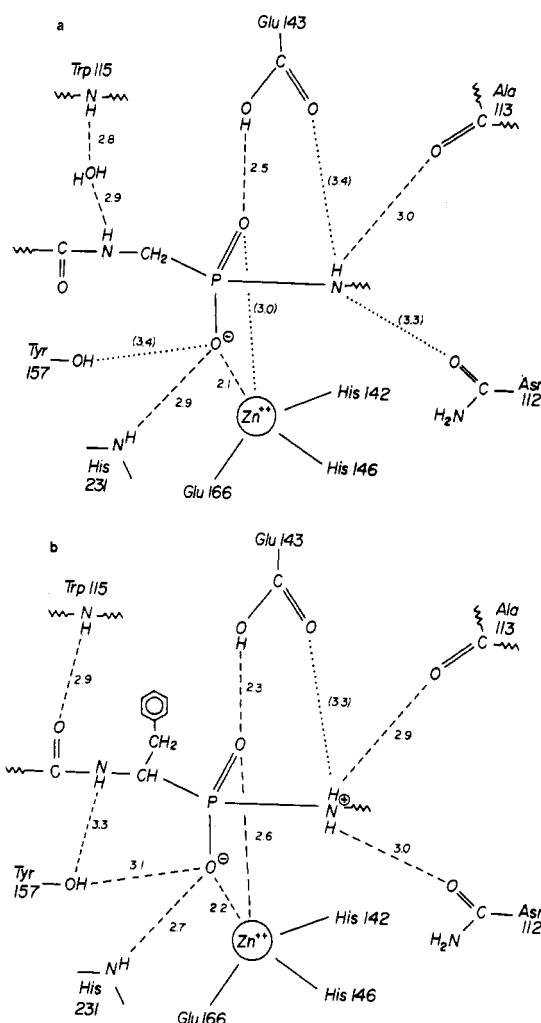

FIGURE 8: Simplified sketch showing the apparent interactions between the two phosphonamidate inhibitors and thermolysin. Presumed hydrogen bonds and interactions with the zinc are drawn as broken lines, other close approaches are shown as dotted lines with the distances in parentheses. (a) ZG^{P}LL. (b) ZF^{P}LA.

and its interactions with the enzyme are presumed to resemble those that occur for a peptide substrate in the transition state. The interactions of the phosphonamide group are of particular interest. One of the phosphonamide oxygens accepts hydrogen bonds from both Tyr-157 and His-231 (Figure 8b). Such hydrogen bonds could stabilize the tetrahedral (hydrated carbon) intermediate during catalysis, analogous to the "oxyanion hole" in the serine proteases [cf. Hangauer et al.
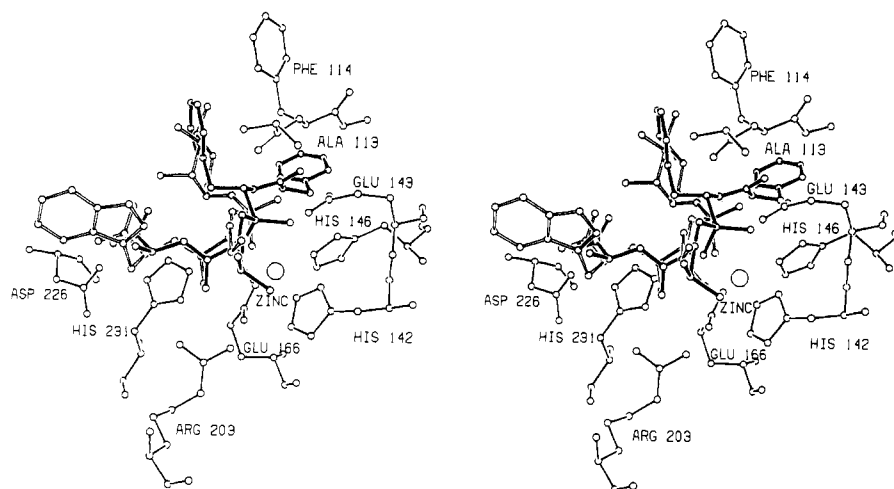
FIGURE 9: Stereoview showing the superposition of phosphoramidon (open bonds) and ZF^{P}LA (solid bonds).

(1984) and Tronrud et al. (1986)]. The second phosphonamide oxygen is very close (2.3 Å) to one of the carboxyl oxygens of Glu-143 (Figure 8b). (The refinement program pushes apart pairs of oxygen atoms only if their interatomic distance is less than 2.3 Å.) The expected pK_a of a phosphonamide group (2.5–3.0) (Oney & Caplow, 1967; Kam et al. 1979) is lower than the typical pK_a of a glutamic acid side chain (ca. 4.5). Therefore, we presume that it is Glu-143 that is protonated in the enzyme–inhibitor complex. The protonated carboxyl then donates a strong hydrogen bond to the phosphonamide oxygen. [Carboxyl oxygens are known to form strong hydrogen bonds with oxygen–oxygen distances as short as 2.4–2.5 Å (Jeffrey & Maluszynska, 1982).] The same type of hydrogen bonding would be expected to occur between Glu-143 and the transition-state intermediate formed by attack of the activated water molecule on the carbonyl carbon (Figure 1). Because the hydrated peptide of the transition state is less bulky than the phosphonamide group, the hydrogen bond between Glu-143 and the transition state could be longer than the value of 2.3 Å observed for ZF^{P}LA.

It is presumed that in the transition state the zinc ion is pentacoordinate (Argos et al., 1978). This was supported by the observation that hydroxamic acid inhibitors show 5-fold coordination (Holmes & Matthews, 1981) and also by the bidentate ligation of N-carboxymethyl peptide inhibitors (Monzingo & Matthews, 1984). In the present study, ZF^{P}LA, the tighter binding inhibitor and the presumed transition-state analogue, also shows 5-fold coordination, whereas ZG^{P}LL, which is presumed to bind in a "nonproductive" mode, has essentially tetrahedral coordination at the metal. Tetrahedral coordination was also observed for the binding of phosphoramidon (Weaver et al., 1977; Tronrud et al., 1986). Zinc–ligand distances for a series of thermolysin–inhibitor complexes are summarized in Table VII. We presume that as the zinc ligation comes closer to full pentacoordination, the phosphorus-containing inhibitors become better approximations to the transition state. The phosphonamide groups of phosphoramidon and ZF^{P}LA are shown superimposed in Figure 9. These are extreme examples from Table VI. ZG^{P}LL is reasonably similar to phosphoramidon, while N-phosphoryl-L-leucinamide (P-Leu-NH$_2$) is intermediate between ZG^{P}LL and ZF^{P}LA (Table VII).

The change in the coordination of the phosphonamide oxygens at the zinc corresponds, in part, to a rotation about the phosphorus–nitrogen bond (Figure 9). This rotation is correlated with an apparent increase in the phosphorus–nitrogen bond length (Table VII), already noted in the comparison of

phosphoramidon with P-Leu-NH$_2$ (Tronrud et al., 1986). [In all the crystallographic refinements the P–N bond was restrained to an "ideal" value of 1.78 Å but, because of the uncertainty of the "expected" value for the bond length, was given a weight of $^1/_9$ relative to all other bonds. See also Tronrud et al. (1986).] The increase in the P–N bond length (Table VII) can be taken as an indication that the nitrogen is becoming cationic. This is also suggested by the decrease in the angle at the nitrogen (from 129° in ZG^{P}LL to 115° in ZF^{P}LA). If, indeed, the phosphonamide nitrogen in ZF^{P}LA is doubly protonated, as seems to be the case, it is yet another attribute of the bound inhibitor as an excellent mimic of the transition state.

Table VII also includes, for the different inhibitors, the distances between the phosphonamide nitrogen and the nearest protein atoms. These distances (and the corresponding directions) show that there are oxygens available (Asn-112 OD1 and the peptide oxygen of Ala-113) to accept two hydrogen bonds from the nitrogen. For ZF^{P}LA and P-Leu-NH$_2$, in which the nitrogen is presumed to be cationic, both these hydrogen bonds are realized. It will also be noted in Table VII that as one proceeds from phosphoramidon to P-Leu-NH$_2$ and ZF^{P}LA, the nitrogen occupies a position closer to Glu-143, consistent with the proposal that Glu-143 is the proton donor. When the two protein oxygens OD1 of Asn-112 and the peptide oxygen of Ala-113 occupy the requisite positions to accept hydrogen bonds from the phosphonamide nitrogen, they exclude solvent. Indeed, the mode of binding adopted by ZF^{P}LA (Figure 6) is such that any access of water to the nitrogen is sterically excluded. Assuming that a substrate adopts a similar configuration, solvent would be excluded from the scissile nitrogen in the same way [also see Hangauer et al. (1984)]. This inaccessibility to solvent argues against water as the proton donor in catalysis, although it is difficult to rule out structural changes that might permit the entry of a water molecule.

As mentioned, the distance in ZF^{P}LA between the phosphonamide nitrogen and one of the oxygens of Glu-143 is 3.3 Å (Figure 8a), consistent with the mechanistic proposal that Glu-143 accepts a proton from the attacking water molecule and subsequently shuttles the proton to the leaving nitrogen of the scissile peptide (Monzingo & Matthews, 1984; Hangauer et al., 1984). By analogy with thermolysin it was proposed that a similar mechanism of action should be considered for carboxypeptidase A (Monzingo & Matthews, 1984). In particular, it was suggested that in carboxypeptidase A the role of the proton donor could be ascribed to Glu-270
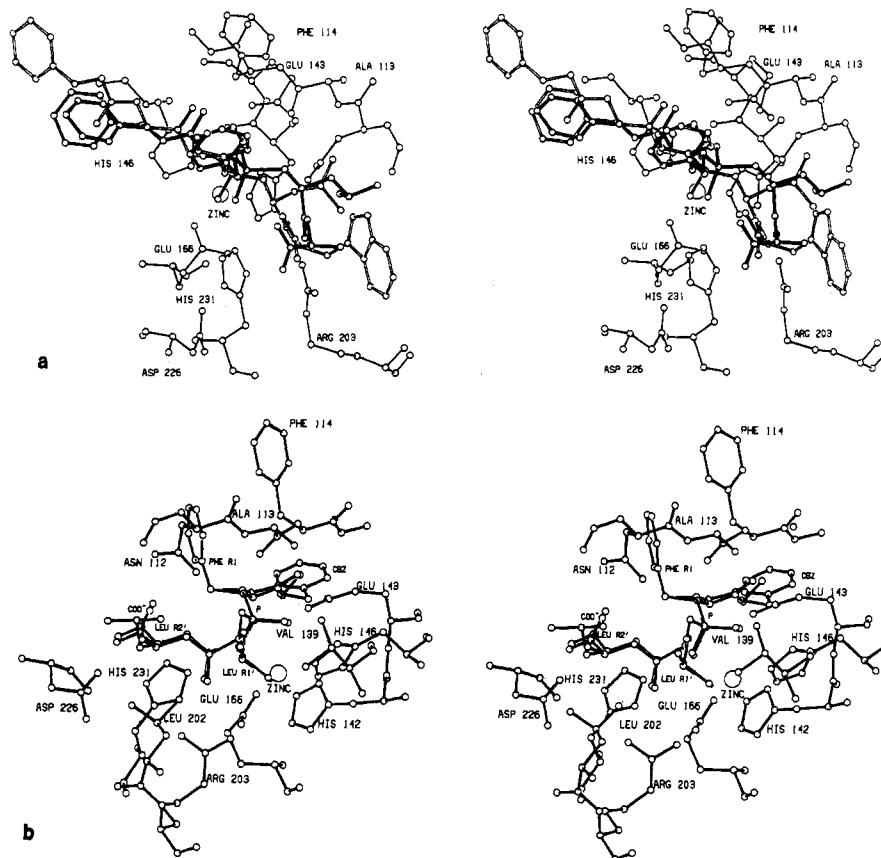
FIGURE 10: (a) Superposition of a model for the presumed transition state (Z-Phe-Phe-Leu-Trp) (Hangauer et al., 1984) (open bonds) on the observed configuration for ZF^{P}LA (solid bonds). For clarity, the protein is drawn with thin bonds. (b) Superposition of a revised model for the transition state (Ala-Phe-Leu-Leu) (see text) on ZF^{P}LA.

rather than Tyr-248. The subsequent demonstration that Tyr-248 of carboxypeptidase A is not essential for catalysis (Gardell et al., 1985) is consistent with the above suggestion and also supports the idea that the mechanisms of action of carboxypeptidase A and thermolysin could be very similar (Kester & Matthews, 1977; Monzingo & Matthews, 1984). Very recently, Christianson and Lipscomb (1986) have reexamined the mode of binding of glycyltryosine to carboxypeptidase A and found that Glu-270 forms a hydrogen bond to the "scissile" nitrogen. This new result is also consistent with the proposed role of Glu-270 as a "proton shuttle" (Monzingo & Matthews, 1984).

On the basis of the observed mode of binding to thermolysin of N-carboxymethyl dipeptide and other inhibitors, Hangauer et al. (1984) used interactive computer graphics to model the presumed intermediates that occur during catalysis. Figure 10a shows the model for the tetrahedral intermediate superimposed on the observed coordinates for ZF^{P}LA. As can be seen, the overall agreement is only moderately good, and there are substantial differences in the binding of the leucine within the S$_1$' "specificity pocket". [The same discrepancy occurred between the proposed transition-state model and the observed binding of "CLT" in the specificity pocket [see Figure 7 of Hangauer et al. (1984)].] Since we believe ZF^{P}LA to be the best model to date for an extended substrate, we have used it as a guide to develop a revised transition-state model (coordinates deposited in the Brookhaven Data Bank). To obtain the model we followed the ZF^{P}LA coordinates as closely as possible except that the geometry of the phosphonamide group was altered to correspond to a hydrated peptide. The "guide positions" for the two oxygen liganded to the zinc were a compromise between the oxygen coordinates observed in "CLT" (Monzingo & Matthews, 1984) and those observed

for ZF^{P}LA. The correspondence between ZF^{P}LA and the revised transition-state model is shown in Figure 10b.

Kinetics of Binding. In general, transition-state inhibitors bind more tightly than ground-state analogues to an enzyme and often bind slowly (Wolfenden, 1976; Frieden et al., 1980; Morrison & Walsh, 1987). Both ZG^{P}LL and ZF^{P}LA were designed specifically as transition-state-analogue inhibitors of thermolysin. Not surprisingly, these two inhibitors have different binding constants, but, unexpectedly, they differ with respect to their binding kinetics (Bartlett & Marlowe, 1983, 1987). ZG^{P}LL has an inhibition constant, K_i, of 9.1 nM and binds normally. On the other hand, ZF^{P}LA, the most potent inhibitor yet reported for thermolysin, demonstrates slow binding kinetics with a K_i of 0.068 nM (Bartlett & Marlowe, 1987). The different properties of ZG^{P}LL and ZF^{P}LA observed in solution can now be correlated with the different modes of binding observed crystallographically.

It is presumed that ZF^{P}LA mimics the transition state in both its bidentate coordination at the zinc and its interactions with the enzyme in the S$_2$, S$_1$, S$_1$', and S$_2$' subsites. ZG^{P}LL is presumed to bind in a mode that would be nonproductive for a substrate. The first question is why the two inhibitors adopt different modes of binding. The presence of the phenylalanine side chain at the R$_1$ position has two consequences. (1) The phenyl group can make more extensive interactions with the enzyme than can a glycine. (2) The phenylalanine side chain restricts rotation about the N–C$_\alpha$ bond much more than is the case with a glycine at this position. The allowed configurations can be evaluated in exactly the same way as for a polypeptide (Ramachandran et al., 1963) except that the trigonal carbonyl group is replaced by the tetrahedral phosphonamide group. The sterically permissible angles of rotation about the N–C$_\alpha$ bond of residue R$_1$ are shown in Figure 11.
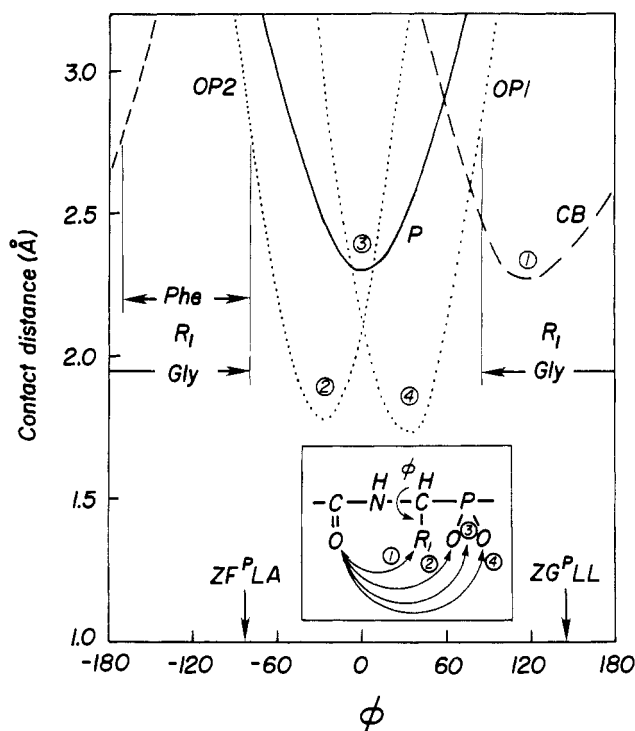
FIGURE 11: Interatomic distances in ZF^{P}LA between the carbonyl oxygen of the carbamate group and, respectively, the phosphorus atom P (solid line), the phosphonamide oxygens OP1 and OP2 (dotted lines), and the β-carbon, CB, of the phenylalanine side chain (dashed line). The boxed insert shows these distances schematically. Each distance is plotted as a function of the rotation, ϕ, of the carbonyl group about the N-C$_\alpha$ (R$_1$) bond (see insert). Assuming that the shortest permissible O$\cdots$O or O$\cdots$C interatomic approach is 2.7 Å (Ramachandran et al., 1963), the allowed ranges of values of ϕ for a glycine and a non-glycine (e.g., phenylalanine) at R$_1$ are as shown in the figure. The observed values for ZG^{P}LL and ZF^{P}LA are also shown.

If R$_1$ is a non-glycine, the dihedral angle ϕ is restricted to the vicinity of $-120°$, with allowed values from about $-170°$ to $-80°$. The observed value for ZF^{P}LA (R$_1 \equiv$ Phe) is $\phi = -83°$. On the other hand, if R$_1$ is a glycine, much greater rotational flexibility is allowed [from about 80° through ±180° to $-80°$ (Figure 11)]. The observed dihedral angle for ZG^{P}LL is $\phi = 146°$. Since the glycine-containing inhibitor could, in principle, adopt the conformation of its phenylalanine counterpart, the differences in the modes of binding of the two inhibitors cannot be attributed to differences in their allowed conformations. Rather, the difference between the binding of ZF^{P}LA and of ZG^{P}LL must be attributed to the additional interactions generated by the phenylalanine side chain. Morihara and Tsuzuki (1970) showed that the K_M for the thermolysin substrate Z-Gly-Leu-Ala is 10.6 mM, whereas Z-Phe-Leu-Ala has a K_M of 0.6 mM. Thus the phenylalanine side chain at the R$_1$ position clearly contributes to binding. In terms of the binding observed for ZF^{P}LA (Figure 6) the phenylalanine side chain lies at an angle to the face of Phe-114, an interaction also seen with other thermolysin inhibitors [e.g., see Kester and Matthews (1977) and Monzingo and Matthews (1984)]. This additional interaction must account for the tighter binding of ZF^{P}LA relative to that of ZG^{P}LL, and, in addition, the different mode of binding. (Because the configuration of ZF^{P}LA in solution is more constrained than that of ZG^{P}LL, there is also an entropic contribution to the tighter binding of ZF^{P}LA relative to that of ZG^{P}LL.) It might also be noted that the substitution of Ala for Leu in the R$_2'$ position is expected to slightly weaken the binding of ZF^{P}LA relative to that of ZG^{P}LL. Morihara and Tsuzuki (1970) found Z-Gly-Leu-Leu to have a K_M of 2.6 mM, whereas Z-Gly-Leu-

Ala has a 4-fold larger value (10.8 mM).

When ZF^{P}LA and ZG^{P}LL bind to thermolysin, each inhibitor displaces a number of solvent molecules. However, there is one water molecule (Sol-362) hydrogen bonded to the peptide nitrogen of Trp-115 that is displaced by ZF^{P}LA (Figure 6) but not by ZG^{P}LL (Figure 5). It is presumed that a substrate displaces Sol-362 and its removal is an obligatory step in the activation of Glu-143 as a nucleophile. Thus, nonblocked dipeptides, which do not displace this solvent atom, are not hydrolyzed by thermolysin (Kester & Matthews, 1977). In contrast, N-acetyl dipeptides are substrates of thermolysin (Morihara et al., 1968) presumably because the acetyl oxygen displaces the solvent molecule from the vicinity of Glu-143.

The difference in the modes of binding of ZG^{P}LL and ZF^{P}LA suggests that the slow binding of the latter inhibitor is associated with the displacement of solvent molecule Sol-362. In native thermolysin, Sol-362 appears to make two relatively long hydrogen bonds, one to the peptide nitrogen of Trp-115 (3.2 Å) and the second to the carboxylate of Glu-143 (also 3.2 Å) (cf. Figure 5). In the complex of thermolysin with ZG^{P}LL, the number of apparent hydrogen bonds to Sol-362 could be as many as four (peptide nitrogen of Trp-115, 2.8 Å; carboxylate of Glu-143, 3.4 Å; inhibitor nitrogen, 2.9 Å; bound solvent Sol2-551, 2.9 Å). Concomitant with the increased number and strength of these hydrogen-bonding interactions, the crystallographic thermal motion parameter, B, for Sol-362 decreases from 31.0 Å^2 in native thermolysin to 9.6 Å^2 in the complex with ZG^{P}LL. This is essentially equal to those of the most well-ordered solvent atoms in the whole structure.

Slow binding has been observed before and is often attributed to the rapid formation of a loose enzyme–inhibitor complex followed by a slow conformational isomerization to a tight complex [e.g., see Wolfenden (1976); Frieden et al. (1980), and Morrison and Walsh (1987)]. The observation that thermolysin has essentially the same conformation in the absence of inhibitors and in complexes with slow and faster binding inhibitors rules out mechanisms in which the enzyme undergoes a substantial conformational change during binding. The possibility that slow binding might require the inhibitor to adopt a rare or energetically unfavorable configuration is also ruled out in the present instance since both ZG^{P}LL and ZF^{P}LA bind with configurations that are readily accessible in solution (Figure 11). In contrast to its analogous substrate, the inhibitor ZF^{P}LA already has tetrahedral geometry before binding occurs. In addition, the tetrahedral phosphonamide group, together with an α-substituent (as in ZF^{P}LA), severely restricts the rotational motion of the carbobenzoxy carbonyl group (Figure 11). In cases such as ZF^{P}LA, where the α-substituent is present, the rotational angle ϕ (Figure 11) is constrained to remain in the vicinity of $-120°$. We presume that the bulky tetrahedral phosphonamide group, together with the carbonyl group in its restricted configuration, occlude the active-site cleft and tend to trap rather than displace the critical solvent molecule. It is presumed that the water molecule has to be substantially displaced from its "rest" position in order for the inhibitor to penetrate the active site. A prebound water molecule could thereby be responsible for slow binding, as has been suggested by Rich (1985) for the binding of pepstatin to the acid proteases. A detailed analysis of possible mechanisms for slow binding, together with additional references, is given by Bartlett and Marlowe (1987) in the following paper in this issue.
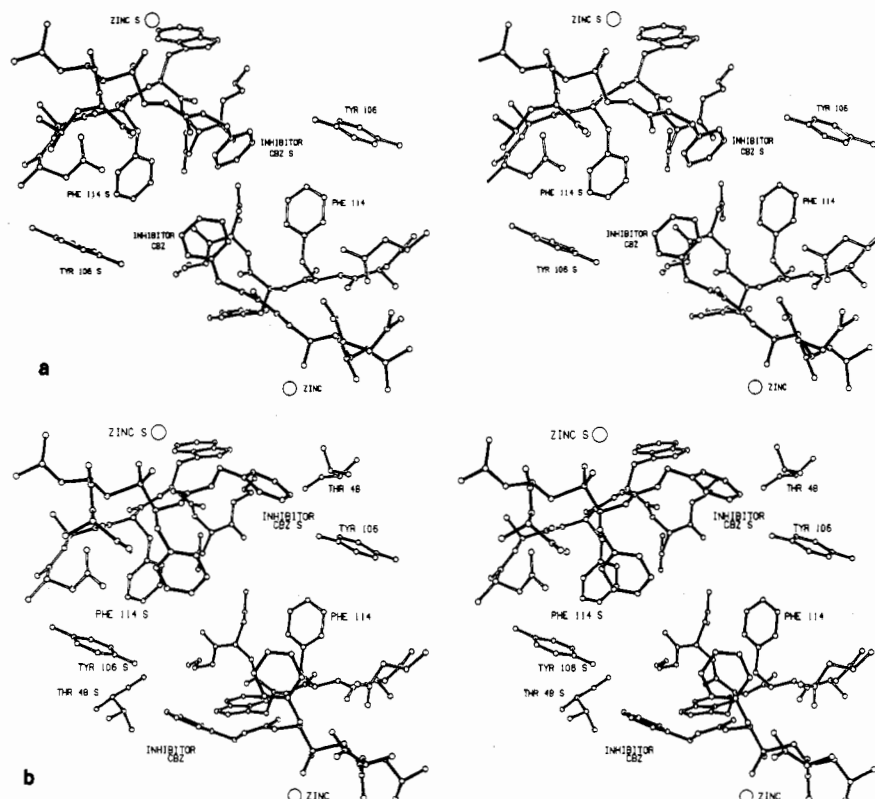
FIGURE 12: Stereo drawings illustrating the potential for steric interference with inhibitors bound in the active site of crystalline thermolysin. Each figure shows one inhibitor molecule (solid bonds) bound in the active site (open bonds) together with a second inhibitor molecule bound to the active site of a neighboring protein molecule. The names of the symmetry-related atoms are followed by an S. The two active sites and the bound inhibitors are related by a crystallographic 2-fold rotational axis that is approximately normal to the plane of the paper. (a) ZG^{P}LL. (b) ZF^{P}LA.

Apart from ZF^{P}LA and its homologues, two other inhibitors of thermolysin have been reported to be slow binders; the first is phosphoramidon, and the second is N-phosphorylleucyl-tryptophan (P-Leu-Trp) (Kam et al., 1979; Kitagishi & Hiromi, 1983, 1984). [Talopepin, a close homologue of phos-phoramidon, also binds slowly (Kitagishi & Hiromi, 1983). See Bartlett and Marlowe (1987) for additional details.] Phosphoramidation does not displace the water molecule at Trp-115 when it binds to thermolysin (Weaver et al., 1977; Tronrud et al., 1986) and, extrapolating from the behavior of N-phosphorylleucine, neither does P-Leu-Trp (Tronrud et al., 1986). Therefore, another reason for the slow binding of these inhibitors must be invoked. The N-phosphoryl-Leu-Trp moiety is common to phosphoramidon and P-Leu-Trp, and it appears that the N-phosphoryl group and the indole groups must both be present to achieve slow binding. Replacement of the tryptophan with phenylalanine, as in N-phosphorylphenyl-alanine, eliminates slow binding (Kam et al., 1979). Similarly, N-(1-carboxy-3-phenylpropyl)leucyltryptophan is a tight-binding inhibitor of thermolysin and retains the tryptophan in the R_2' position but lacks the phosphoryl group and binds with normal kinetics (Maycock et al., 1981). Further studies will be required before an explanation for the slow binding of P-Leu-Trp and phosphoramidon can be provided. Kam et al. (1979) have proposed that the slow binding might be due to a slow conformational change of the protein in the vicinty of Asn-112, but the observed structural changes are small and there is no obvious reason why they could not occur rapidly. One special characteristic of these inhibitors is that the ni-trogen of the tryptophan side chain makes a hydrogen bond with the backbone carbonyl oxygen of Asn-111 (Weaver et al., 1977; Monzingo & Matthews, 1984). Whether the com-bination of the phosphoryl group and the tryptophan in P-

Leu-Trp and phosphoramidon promote slow binding by pre-venting facile displacement of solvent remains to be tested.

Crystal Packing and Steric Hindrance. In considering the different modes of binding of the two inhibitors, there is an-other potential complication that needs to be discussed, namely, steric limitations imposed by the packing of the thermolysin molecules in the crystal. On one hand, the observation that bulky inhibitors such as ZF^{P}LA and phosphoramidon can be bound to crystalline thermolysin shows that the active site is relatively accessible. On the other hand, consideration of the molecular packing within the crystals shows that there is the possibility of steric interference for inhibitors occupying the S_2 and S_3 subsites. These potential steric limitations can be of two types, either an inhibitor bound to one thermolysin molecule can clash with another thermolysin molecule or in-hibitor molecules bound to two active sites may interfere with each other.

The situation for ZF^{P}LA is shown in Figure 12b. The closest "intermolecular" approach is 3.5 Å and is between the carbobenzoxy group of the inhibitor and Thr-48 of a 2-fold-related thermolysin molecule. This distance is just beyond the range of significant van der Waals interactions, although it does not exclude possible indirect effects mediated via bound solvent molecules. However, since there is no direct steric clash between ZF^{P}LA and any other protein or inhibitor molecule in its neighborhood, it is reasonable to assume that the mode of binding of ZF^{P}LA seen in the crystals is very similar to that in solution.

For ZG^{P}LL the potential intermolecular contacts are somewhat different (Figure 12a). Here the carbobenzoxy group of one bound inhibitor comes within 3.5 Å of the car-bobenzoxy group of another inhibitor molecule bound to the 2-fold-related thermolysin molecule. There are also some

approaches of 3.8–4.0 Å between the carbobenzoxy group and Phe-114 of a neighboring thermolysin molecule. However, as with ZF^{P}LA, these distances all appear to be too long to suggest direct intermolecular interactions. Thus, both ZF^{P}LA and ZG^{P}LL come within the vicinity of neighboring molecules in the crystal, but in neither case is there evidence that these neighboring molecules sterically interfere with the preferred mode of binding.

One observation that led us to be concerned about possible steric interference was the discrepancy between the electron density at the phosphorus positions in the respective difference maps (Figures 3 and 4). The peak density for ZF^{P}LA is about 60% that for ZG^{P}LL, suggesting that ZF^{P}LA might be bound to the enzyme with less than 100% occupancy. To test this possibility, we refined the occupancy parameters of two models. In the first model the active site contained a molecule of ZF^{P}LA in which the occupancies of all the atoms were constrained to be equal. The second model included, in addition, the solvent molecules that are displaced when the inhibitor is bound. The solvent atoms were constrained to have equal occupancies but were not tied to the occupancy of the inhibitor. Both calculations lead to the conclusion that ZF^{P}LA occupies the active sites of 80–85% of the thermolysin molecules in the crystal phase. As a control, similar calculations were carried out for ZG^{P}LL and led to an inhibitor occupancy of 100%. The difference in occupancy might explain why the thermal factors of ZF^{P}LA are consistently higher than those of ZG^{P}LL (Table IV). Since the parameters for ZF^{P}LA given in Table IV were obtained by assuming 100% occupancy for the inhibitor, the thermal factors would tend to increase to compensate for any loss of electron density due to partial occupancy.

ACKNOWLEDGMENTS

REFERENCES

Antonov, V. K., Ginodman, L. M., Rumsh, L. D., Kapitannikov, Y. V., Barshevskaya, T. N., Yavashev, L. P., Gurova, A. G., & Volkova, L. I. (1981) Eur. J. Biochem. 117, 195–200.

Argos, P., Garavito, R. M., Eventoff, W., Rossmann, M. G., & Brändén (1978) J. Mol. Biol. 126, 141–158.

Bartlett, P. A., & Marlowe, C. K. (1983) Biochemistry 22, 4618–4624.

Bartlett, P. A., & Marlowe, C. K. (1987) Biochemistry (following paper in this issue).

Bolognesi, M. C., & Matthews, B. W. (1979) J. Biol. Chem. 254, 634–639.

Bowen, H. J. M., Donohue, J., Jenkin, D. G., Kennard, O., Wheatley, P. J., & Whiffen, D. H. (1958) Tables of Interatomic Distances and Configuration in Molecules and Ions (Mitchell, A. D., & Cross, L. C., Eds.) The Chemical Society, London.

Christianson, D. W., & Lipscomb, W. N. (1986) Proc. Natl. Acad. Sci. U.S.A. 83, 7568–7572.

Frieden, C., Kurz, L. C., & Gilbert, H. R. (1980) Biochemistry 19, 5303–5309.

Galardy, R. E. (1982) Biochemistry 21, 5777–5781.

Galardy, R. E., Kontoyiannidou-Ostrem, Y., & Kortylewicz, Z. P. (1983) Biochemistry 22, 1990–1995.

Gardell, S. J., Craik, C. S., Hilvert, D., Urdea, M. S., & Rutter, W. J. (1985) Nature (London) 317, 551–554.

Hangauer, D. G., Monzingo, A. F., & Matthews, B. W. (1984) Biochemistry 23, 5730–5741.

Holmes, M. A., & Matthews, B. W. (1981) Biochemistry 20, 6912–6920.

Holmes, M. A., & Matthews, B. W. (1982) J. Mol. Biol. 160, 623–639.

Holmes, M. A., Tronrud, D. E., & Matthews, B. W. (1983) Biochemistry 22, 236–240.

Holmquist, B. (1977) Biochemistry 16, 4591–4594.

Holmquist, B., & Vallee, B. L. (1979) Proc. Natl. Acad. Sci. U.S.A. 76, 6216–6220.

Jack, A., & Levitt, M. (1971) Acta Crystallogr., Sect. A: Cryst. Phys., Diffr., Theor. Gen. Crystallogr. A34, 931–935.

Jacobsen, N. E., & Bartlett, P. A. (1981) J. Am. Chem Soc. 103, 654–657.

Jeffrey, G. A., & Maluszynska, H. (1982) Int. J. Biol. Macromol. 4, 173–185.

Kam, C.-M., Nishino, N., & Powers, J. C. (1979) Biochemistry 18, 3032–3038.

Kester, W. R., & Matthews, B. W. (1977) Biochemistry 16, 2506–2516.

Kitagishi, K., & Hiromi, K. (1983) J. Biochem. (Tokyo) 93, 55–59.

Kitagishi, K., & Hiromi, K. (1984) J. Biochem. (Tokyo) 95, 529–534.

Kojima, T., Yamane, T., & Ashida, T. (1978) Acta Crystallogr., Sect. B: Struct. Crystallogr. Cryst. Chem. B34, 2896–2898.

Komiyama, T., Suda, H., Aoyagi, T., Takeuchi, T., & Umezawa, S. (1975) Arch. Biochem. Biophys. 171, 727–731.

Kunugi, S., Hirohara, H., & Ise, N. (1982) Eur. J. Biochem. 124, 157–163.

Matthews, B. W., Weaver, L. H., & Kester, W. R. (1974) J. Biol. Chem. 249, 8030–8044.

Maycock, A. L., DeSousa, D. M., Payne, L. G., ten Broeke, J., Wu, M. T., & Patchett, A. A. (1981) Biochem. Biophys. Res. Commun. 102, 963–969.

Monzingo, A. F., & Matthews, B. W. (1982) Biochemistry 21, 3390–3394.

Monzingo, A. F., & Matthews, B. W. (1984) Biochemistry 23, 5724–5729.

Morihara, K., & Tsuzuki, H. (1970) Eur. J. Biochem. 15, 374–380.

Morihara, K., Tsuzuki, H., & Oka, T. (1968) Arch. Biochem. Biophys. 123, 572–588.

Morrison, J. F., & Walsh, C. T. (1987) Adv. Enzymol. Relat. Areas Mol. Biol. (in press).

Nishino, N., & Powers, J. C. (1979) J. Biol. Chem. 255, 3482–3486.

Oney, L., & Caplow, M. (1967) J. Am. Chem. Soc. 89, 6972–6980.

Pangburn, M. K., & Walsh, K. A. (1975) Biochemistry 14, 4050–4054.

Pauling, L. (1946) Chem. Eng. News 24, 1375–1377.

Ramachandran, G. N., Ramakrishnan, C., & Sasisekharan, V. (1963) J. Mol. Biol. 7, 95–99.

Rich, D. H. (1985) J. Med. Chem. 28, 263–273.

Rossmann, M. G. (1979) J. Appl. Crystallogr. 12, 225–238.

Schmid, M. F., Weaver, L. H., Holmes, M. A., Grütter, M. G., Ohlendorf, D. H., Reynolds, R. A., Remington, S. J., & Matthews, B. W. (1981) Acta Crystallogr., Sect., A: Cryst Phys., Diffr., Theor. Gen. Crystallogr. A37, 701–710.

Suda, H., Aoyagi, T., Takeuchi, T., & Umezawa, H. (1973) J. Antibiot. 26, 621–623.

Thorsett, E. D., Harris, E. E., Peterson, E. R., Greenlee, W. J., Patchett, A. A., Ulm, E. H., & Vassil, T. C. (1982) *Proc. Natl. Acad. Sci. U.S.A. 79*, 2176–2180.

Tronrud, D. E., Monzingo, A. F., & Matthews, B. W. (1986) *Eur. J. Biochem. 157*, 261–268.

Tronrud, D. E., Holden, H. M., & Matthews, B. W. (1987a) *Science (Washington, D.C.) 235*, 571–574.

Tronrud, D. E., Ten Eyck, L. F., & Matthews, B. W. (1987b) *Acta Crystallogr., Sect. A: Found. Crystallogr. A43*, 489–501.

Weaver, L. H., Kester, W. R., & Matthews, B. W. (1977) *J. Mol. Biol. 114*, 119–132.

Wolfenden, R. (1976) *Annu. Rev. Biophys. Bioeng. 5*, 271–306.

Possible Role for Water Dissociation in the Slow Binding of Phosphorus-Containing Transition-State-Analogue Inhibitors of Thermolysin[†]

Paul A. Bartlett* and Charles K. Marlowe

Department of Chemistry, University of California, Berkeley, California 94720

Received May 18, 1987; Revised Manuscript Received August 6, 1987

ABSTRACT: A number of phosphonamidate and phosphonate tripeptide analogues have been studied as transition-state-analogue inhibitors of the zinc endopeptidase thermolysin. Those with the form Cbz-Gly^P(Y)Leu-X [ZG^P(Y)LX, X = NH$_2$ or amino acid, Y = NH or O linkage] are potent (K_i = 9–760 nM for X = NH, 9–660 μM for X = O) but otherwise ordinary in their binding behavior, with second-order rate constants for association (k_{on}) greater than 10^5 M^{-1} s^{-1}. Those with the form Cbz-X^P(Y)-Leu-Ala [ZX^P(Y)LA, X^P = α-substituted phosphorus amino acid analogue] are similarly potent (K_i for ZF^{P}LA = 68 pM) but slow binding ($k_{on} \leq 1300$ M^{-1} s^{-1}). Several kinetic mechanisms for slow binding behavior are considered, including two-step processes and those that require prior isomerization of inhibitor or enzyme to a rare form. The association rates of ZF^{P}LA and ZF^P(O)LA are first order in inhibitor concentration up to 1–2 mM, indicating that any loose complex along the binding pathway must have a dissociation constant above this value. The crystallographic investigation described in the preceding paper [Holden, H. M., Tronrud, D. E., Monzingo, A. F., Weaver, L. H., & Matthews, B. W. (1987) *Biochemistry* (preceding paper in this issue)] identifies a specific water molecule in the active site that may hinder binding of the α-substituted inhibitors. The implication of this observation for a mechanism for slow binding is discussed.

Enzyme inhibitors have been used to study the importance of metabolic pathways and the role of individual enzymes, to shed light on enzyme mechanisms, and to aid in the development of useful pharmacological and agricultural agents. In contrast to investigations of enzyme–substrate interactions, which generally focus on the *kinetic* details of the process, most studies of enzyme inhibitors have focused on the *thermodynamic* aspects of the binding phenomenon. Of interest in the latter regard are the protein–inhibitor contacts that contribute incrementally to overall affinity, the interplay between inhibitor potency and its relevance to the enzyme mechanism, or the potential of an inhibitor as a pharmaceutical agent. However, with greater refinement in the design of potent and mechanistically relevant inhibitors, there is increasing interest in the kinetic details of their binding behavior (Frieden, 1970; Cha, 1975, 1976; Williams & Morrison, 1979; Duggleby et al., 1982; Morrison & Walsh, 1987; Kurz et al., 1987). This interest stems in great measure from the increasing frequency with which "slow binding behavior" is observed, that is, instances in which formation of an enzyme–inhibitor complex takes place at a rate considerably slower than expected for a diffusion-limited process. In spite of increasing interest in this behavior, there remains limited insight into the molecular basis of the phenomenon, either in the form of direct evidence to support the varied explanations proposed or through the

identification of the responsible structural elements in the inhibitors themselves. In this paper, we describe the behavior of a series of inhibitors of the zinc endopeptidase thermolysin and the identification of a specific element in their structure that produces slow binding behavior. In the preceding paper, Holden et al. (1987) present a crystallographic comparison of the structures of thermolysin complexes with representative slow- and fast-binding inhibitors and identify what may be the key element in the slow binding process.

Thermolysin, a 34.6-kDa, zinc-containing endopeptidase isolated from *Bacillus thermoproteolyticus*, is important as one of the prototypical metalloproteases and a model for the more pharmacologically important members of this class (Cushman & Ondetti, 1981; Maycock et al., 1981; Hangauer et al., 1984; Hersh & Morihara, 1986). Its substrate specificity, including its selectivity for hydrophobic amino acids at the P$_1$ and P$_1'$ sites (Schechter & Berger, 1967), has been well characterized (Morihara & Tsuzuki, 1970; Morgan & Fruton, 1978; Hersh & Morihara, 1986), and it has been the focus of a number of inhibitor (Maycock et al., 1981; Bartlett & Marlowe, 1983; Shenvi & Kettner, 1985, and references cited therein) and crystallographic studies (Monzingo & Matthews, 1984; Tronrud et al., 1986, 1987, and references cited therein). The most recent proposal with respect to its mechanism is that of Hangauer, Monzingo, and Matthews (1984), who incorporated both kinetic and structural information in suggesting a sequence involving attack of the zinc-bound water on the scissile carbonyl group, with simultaneous coordination of the carbonyl oxygen to the metal. Key

* Author to whom correspondence should be addressed.